



Available online at [www.sciencedirect.com](http://www.sciencedirect.com)

ScienceDirect

European Journal of Protistology 73 (2020) 125669

European Journal of  
PROTISTOLOGY

[www.elsevier.com/locate/ejop](http://www.elsevier.com/locate/ejop)

# Morphology, morphogenesis, and molecular phylogeny of a new freshwater ciliate, *Gonostomum jangbogoensis* n. sp. (Ciliophora, Hypotricha), from Victoria Land, Antarctica

Kyung-Min Park<sup>a,b,c,1</sup>, Jae-Ho Jung<sup>d,1</sup>, Jeong-Hoon Kim<sup>a</sup>, Gi-Sik Min<sup>b</sup>, Sanghee Kim<sup>a,\*</sup>

<sup>a</sup>Division of Polar Life Sciences, Korea Polar Research Institute, Incheon 21990, South Korea

<sup>b</sup>Department of Biological Sciences, Inha University, Incheon 22212, South Korea

<sup>c</sup>Department of Biological Resources Research, National Institute of Biological Resources, Incheon 22689, South Korea

<sup>d</sup>Department of Biology, Gangneung-Wonju National University, Gangneung 25457, South Korea

Received 4 March 2019; received in revised form 17 December 2019; accepted 22 December 2019

Available online 3 January 2020

## Abstract

In a study on ciliate diversity, we discovered the new hypotrich species, *Gonostomum jangbogoensis* n. sp., in freshwater from Terra Nova Bay, Victoria Land, southeast Antarctica. We describe its morphology and morphogenesis using standard methods, and the SSU rRNA gene phylogeny is provided as well. Morphology of *Gonostomum jangbogoensis* n. sp. is characterized as follows: slender to elongated body shape; grayish under low magnification; cortical granules present; 32–41 adoral membranelles; 3 enlarged frontal cirri; 1 buccal cirrus; 2 frontoterminal cirri; 3 or 4 frontoventral cirral pairs, 2 pretransverse cirri, 6–7 transverse cirri; 13–19 left and 18–26 right marginal cirri; 17–23 paroral kinetids; 3 dorsal kinetics; 3 caudal cirri; 2 macronuclear nodules with 1–3 micronuclei. The morphogenesis of the new species confirms that it has at least seven frontal-ventral-transverse cirral anlagen, which is also reported in *Gonostomum* sp. 1 sensu Shin from Korea. Even though these two populations occur very far from each other, the morphometric data prove that this character state, the seven cirral anlagen, is a stable feature across these populations and might be an apomorphy. The phylogenetic analyses show that the genus *Gonostomum* is non-monophyletic and that the new species is a sister to *G. bromelicola*.

© 2020 Elsevier GmbH. All rights reserved.

**Keywords:** Ciliophora; Gonostomatidae; Ontogenesis; SSU rRNA gene; Taxonomy

## Introduction

Victoria Land is one of the largest ice-free regions in continental Antarctica, covering the area from Darwin Glacier to Cape Adare at a latitudinal gradient of 8°. The Transantarctic Mountains, low-elevation coastal areas, and desert environ-

ments can be all found in this region (Kim et al. 2015). Many lakes, ponds, and streams in Antarctica lie between the longitudes of 150 °E and 150 °W; however, crustacean zooplankton and common aquatic taxa are conspicuously absent there due to the extreme environment in these aquatic ecosystems. Antarctic water bodies are thus inhabited by a small number of species of microscopic life-forms (Vincent and James 1996).

Ciliates are globally distributed in a variety of habitats such as soil, freshwater, and seawater and are one of the most

\*Corresponding author.

E-mail address: [sangheekim@kopri.re.kr](mailto:sangheekim@kopri.re.kr) (S. Kim).

<sup>1</sup>Co-first authors.

species-rich groups within protists (Lynn 2008; Russell et al. 2016). Ciliates are widely used as bioindicators, with a relatively prompt response based on their delicate membranes and fast growth (e.g., Berger and Foissner 2003; Foissner et al. 1991; Jiang et al. 2011, 2013; Xu et al. 2014).

The genus *Gonostomum* Sterki, 1878 is characterized by an adoral zone in *Gonostomum* pattern, three bipolar dorsal kinetics, and the presence of caudal cirri (Berger 2011). It is the type genus of the Gonostomatidae Small and Lynn, 1985 and comprises 17 species including two invalid species: 1) *G. affine* (Stein, 1859) Sterki, 1878, type species; 2) *G. strenuum* (Engelmann, 1862) Sterki, 1878; 3) *G. algicola* Gellért, 1942; 4) *G. kuehnelti* Foissner, 1987; 5) *G. namibiense* Foissner et al., 2002; 6) *G. albicarpathicum* Vd'ačný and Tirjaková, 2006; 7) *G. singhii* Kamra et al., 2008; 8) *G. paronense* Bharti et al., 2015, invalid species according to ICZN (2012, Article 8.5.3); 9) *G. bromelicola* Foissner, 2016; 10) *G. fraterculus* Foissner, 2016; 11) *G. halophilum* Foissner, 2016; 12) *G. lajacola* Foissner, 2016; 13) *G. multinucleatum* Foissner, 2016; 14) *G. salinarum* Foissner, 2016; 15) *G. caudatulum* Foissner and Heber in Foissner, 2016; 16) *G. sinicum* Lu et al., 2017; and 17) *Gonostomum* sp. 1 sensu Shin (1994). Of these species, *G. affine* and *G. kuehnelti* were recorded in Antarctica (Berger 2011; Foissner 1998). Further, among these species, *Gonostomum* sp. 1 sensu Shin (1994) is deemed to have a seventh frontal-ventral-transverse cirral anlage that is not observed in the type species (Berger 2011). Phylogenetic analyses show that *Gonostomum affine* + *G. strenuum* + *G. bromelicola* + *G. jangbogoensis* + *G. sinicum* cluster with *Paragonostomoides xianicum* and *Cotterillia bromelicola* based on small subunit ribosomal DNA sequence and hence the genus *Gonostomum* is non-monophyletic (Lu et al. 2017; Wang et al. 2017).

In this study, we report a new freshwater *Gonostomum*, *G. jangbogoensis* n. sp., collected from Terra Nova Bay, Victoria Land, southeast Antarctica based on live observations, protargol-preparations, and SSU rRNA gene sequencing.

## Material and methods

### Sample collection and identification

The sample was collected from a freshwater pond near the Jang Bogo Station ( $74^{\circ}37'58.76''S$ ,  $164^{\circ}13'35.84''W$ ), Terra Nova Bay, Victoria Land, southeast Antarctica, in February 2014. Water and sediment samples were collected under the ice surface of the pond. The sediment of the pond was composed of small stones and sand. The sample was transferred to the laboratory of the Jang Bogo Station on Terra Nova Bay. It was stored at  $4^{\circ}C$  during the 4-month transport by a ship and was cultured at  $4^{\circ}C$  after arriving at the Korea Polar Research Institute (KOPRI), Incheon, South Korea. All morphological and molecular analyses were based on specimens from non-clonal raw cultures.

Live specimens were observed under a light microscope (Zeiss Axio Imager 2; Carl Zeiss, Oberkochen, Germany) at  $50\times$  to  $1000\times$  magnification and a stereo microscope (Leica M205 C; Leica Microsystems, Wetzlar, Germany). Protargol impregnation was performed according to “Procedure A” described by Foissner (2014). The protargol was synthesized according to Pan et al. (2013). Drawings of live specimens were based on free-hand sketches and photomicrographs, while those from protargol-prepared individuals were made with a drawing device using Illustrator (Adobe, San Jose, CA, USA). Counts and measurements on protargol-impregnated specimens were performed at  $400\times$  and  $1000\times$  magnification using an image analyzer (AxioVision SE64 Rel. 4.9.1; Carl Zeiss). General terminology is according to Berger (2011).

### SSU rRNA gene sequencing

A single specimen of the new species was washed several times with distilled water to remove any contaminants (i.e., eukaryotes). Genomic DNA was extracted using a RED-Extract-N-Amp Tissue PCR Kit (Sigma, St. Louis, MO, USA) following the manufacturer’s instructions. The conditions for PCR were as follows: initial denaturation at  $94^{\circ}C$  for 3 min; 40 cycles of denaturation at  $95^{\circ}C$  for 15 s, annealing at  $58^{\circ}C$  for 30 s, and extension at  $72^{\circ}C$  for 4 min; and a final extension step at  $72^{\circ}C$  for 7 min. The almost complete small subunit ribosomal RNA (SSU rRNA) gene was amplified using two primers: slightly modified New EukA (5'-CTG GTT GAT YCT GCC AGT-3') and LSU rev3 (5'-GCA TAG TTC ACC ATC TTT CG-3') (Sonnenberg et al. 2007). The PCR product was purified using a QIAquick PCR Purification Kit (Qiagen, Hilden, Germany). Two internal primers were used for sequencing: 18S + 810 (5'-GCC GGA ATA CAT TAG CAT GG-3') and 18S-300 (5'-CAT GGT AGT CCA ATA CAC TAC-3') (Jung et al. 2011). DNA sequencing was performed using an ABI 3700 sequencer (Applied Biosystems, Foster City, CA, USA).

### Phylogenetic analyses

To analyze the phylogenetic position of *Gonostomum jangbogoensis* n. sp., the SSU rRNA gene sequences of 56 species were used. The oligotrichs *Strombidium styliferum* and *S. sulcatum* were selected as the outgroup. GenBank accession numbers follow the species names in the phylogenetic tree (Fig. 5).

The sequences were aligned using Clustal X 1.81 (Jeanmougin et al. 1998) and were manually trimmed at both ends using BioEdit 7.1.11 (Hall 1999). The alignment was further visually checked. A best-fit substitution model for the phylogenetic analyses was chosen using jModelTest 2.1.7 (Darriba et al. 2012). The model GTR + I (0.6810) + G (0.5470) was selected under the Akaike information criterion (AIC). The Bayesian inference (BI) tree was generated by

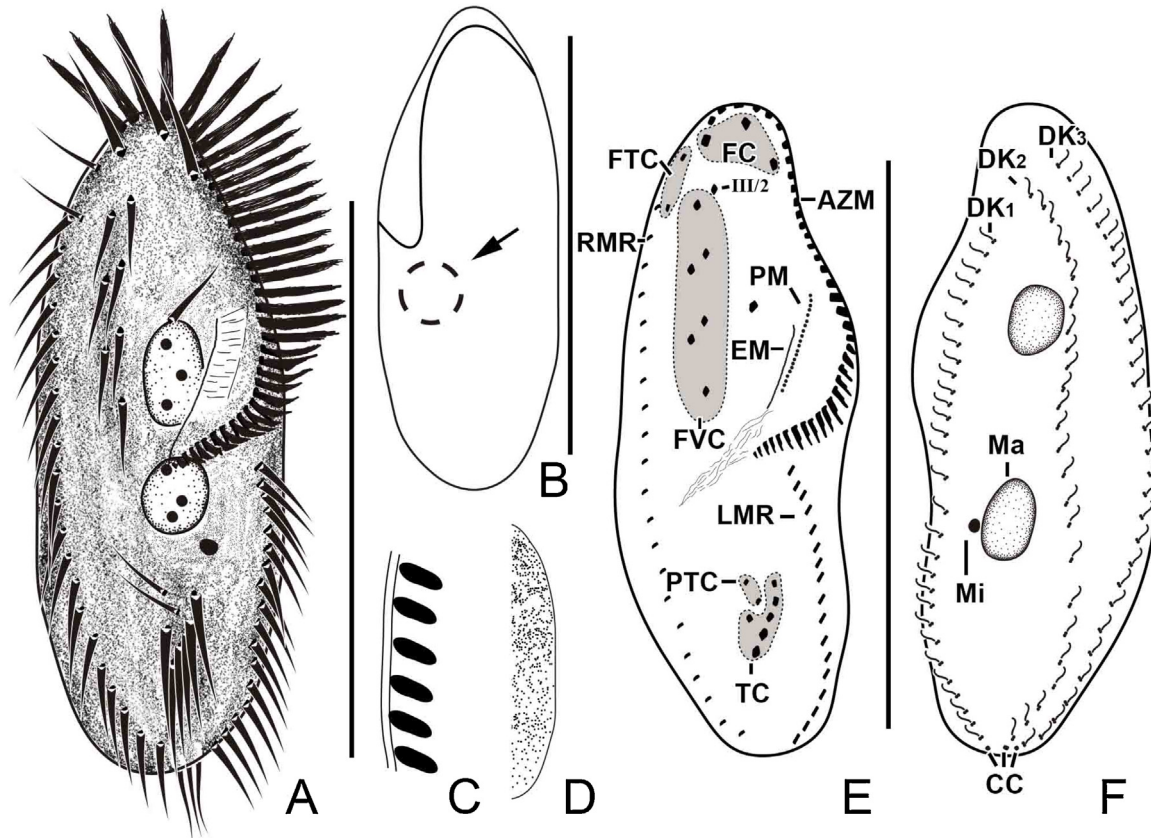


**Fig. 1.** A–F. *Gonostomum jangbogoensis* n. sp. in life (A, B) and after protargol preparation (C, D). A: Ventral view of a representative specimen. B: Dorsal view showing contractile vacuole (arrow). C: Cortical granules,  $2.0\text{--}2.5 \times 0.5\text{--}0.7 \mu\text{m}$  in size. D: Dorsal view showing distribution of cortical granules. E, F: Ciliature of ventral and dorsal side and nuclear apparatus of holotype. AZM, adoral zone of membranelles; CC, caudal cirri; CV, contractile vacuole; DK<sub>1–3</sub>, dorsal kineties; EM, endoral membrane; FC, frontal cirri; FTC, frontoterminal cirri; FVC, frontoventral cirri; LMR, left marginal row; Ma, macronucleus nodule; Mi, micronucleus; RMR, right marginal row; PM, paroral membrane; PTC, pretransverse cirri; TC, transverse cirri. Scale bars: 100  $\mu\text{m}$ .

MrBayes 3.2.5 (Ronquist et al. 2012) using the Markov Chain Monte Carlo (MCMC) simulation for 1,000,000 generations, with a burn-in of 300,000. The maximum likelihood (ML) analysis was conducted using PhyML version 3.1 (Guindon et al. 2010) with the GTR + I + G evolutionary model and 1000 bootstrap replicates.

For interpretation of bootstrap values, the methodology of Vd'ačný and Rajter (2015) was followed:  $\geq 95$ , high support; 71–94, moderate support; 50–70, low support; and <50, no support (Hillis and Bull 1993). Bayesian posterior probability values were considered in the following manner: <0.95 as low;  $\geq 0.95$  as high (Alfaro et al. 2003).

The best (i.e. unconstrained) tree and the topologically constrained trees were inferred in PAUP\* v4.0b10 (Swofford 2003), using ML criterion and a heuristic search with SPR branch swapping and 10 random sequence addition replicates. The log likelihoods of the best and constrained ML trees under the best-fit model were calculated with the “lset” command in PAUP\*. The following topologies were statistically tested: Monophyly of gonostomatids (*Gonostomum* spp. + *Cotterillia* + *Paragonostomoides*), monophyly of all *Gonostomum* spp., and monophyly of all *Gonostomum*

spp. except for *G. namibiense* and *G. paronense*. Hasegawa topological tests (as implemented in the CONSEL package (Shimodaira and Hasegawa 2001)) were used to test statistical significance of the topological constraint.

## ZooBank registration

ZooBank registration number of present work (see Recommendation 8A of ICBN 2012): urn:lsid:zoobank.org:pub:565D3142-3C8E-4D68-931C-2270BCB5D277.

## Results

*Gonostomatidae* Small and Lynn, 1985

*Gonostomum* Sterki, 1878

*Gonostomum jangbogoensis* n. sp.

**Diagnosis:** Body size in vivo  $95\text{--}135 \times 40\text{--}55 \mu\text{m}$ . Body elliptical, flexible but not contractile; grayish under low magnification. Cortical granules rod-shaped, colorless. 2 macronuclear nodules, 1–3 micronuclei. 32–41 adoral mem-

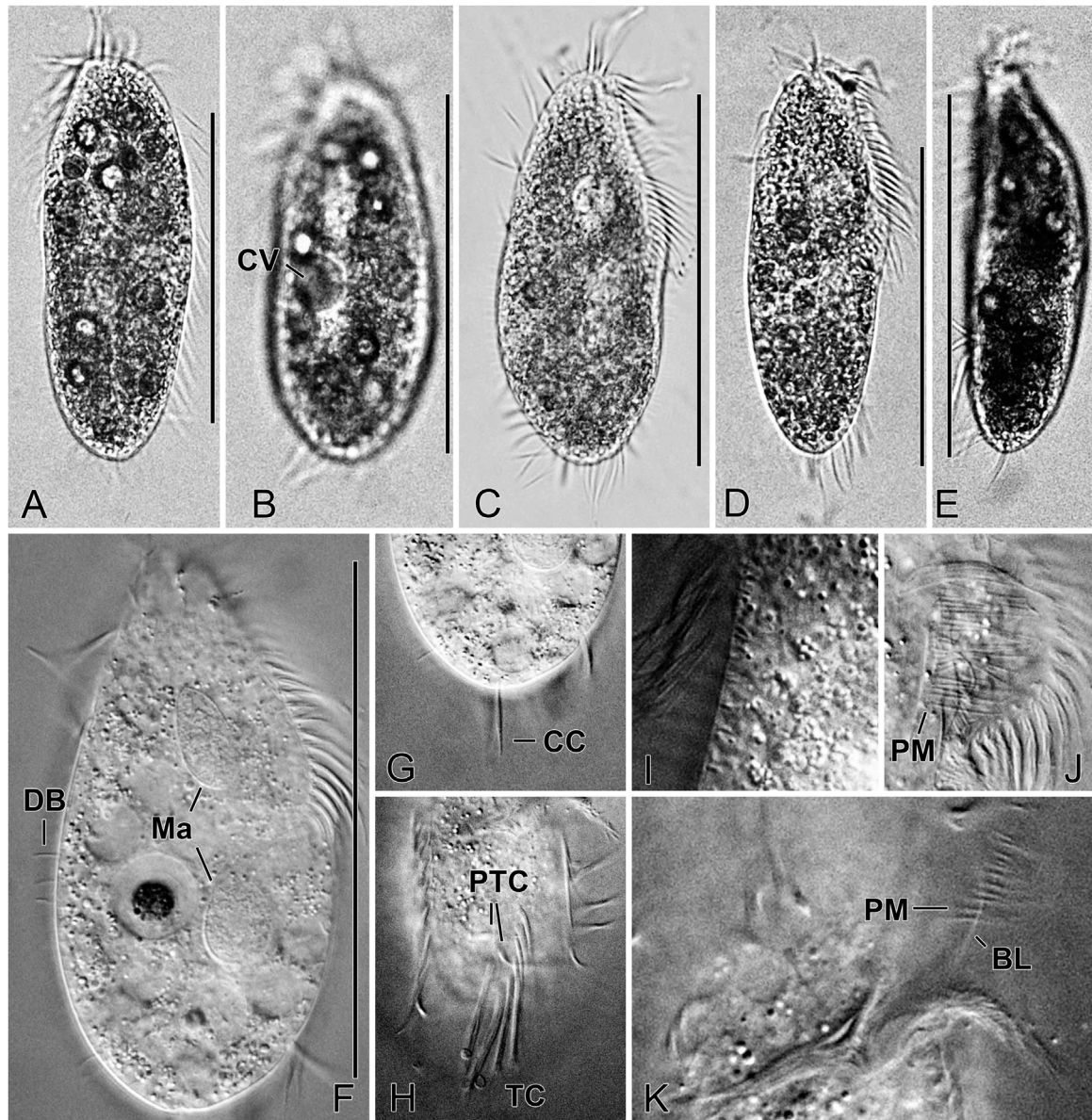


**Fig. 2.** A–K. *Gonostomum jangbogoensis* n. sp., photomicrographs in life (differential interference contrast). A, B: Dorsal views. C, D: Ventral view of a wide and a slender specimen. E: Left lateral view. F: Ventral view of a slightly squeezed specimen showing macronuclear nodules and dorsal cilia. G: Dorsal view showing caudal cirri. H: Specimen with two pretransverse and seven transverse cirri. I: Dorsal view showing cortical granules. J: Paroral membrane. K: Paroral membrane and buccal lip. BL, buccal lip; CC, caudal cirri; CV, contractile vacuole; DB, dorsal bristles; Ma, macronucleus nodule; PM, paroral membrane; PTC, pretransverse cirri; TC, transverse cirri. Scale bars: 100  $\mu\text{m}$ .

branelles, 3 frontal cirri, 1 buccal cirrus, 2 frontoterminal cirri, 3 or 4 frontoventral cirral pairs, 2 pretransverse cirri, 6 or 7 transverse cirri, 13–19 left and 18–26 right marginal cirri. Paroral composed of 17–23 widely spaced monokinetids. 3 dorsal kineties, 3 caudal cirri.

**Type locality:** Pond near Jang Bogo Station, Terra Nova Bay, Victoria Land, southeast Antarctica ( $74^{\circ}37'58.76''\text{S}$ ,  $164^{\circ}13'35.84''\text{W}$ ).

**Type material:** The slide (ACNS000202) containing the holotype specimen (Fig. 1E, F) and three paratype slides (ACNS000201, ACNS000203, ACNS000204) with

protargol-impregnated specimens are deposited in the Korean Polar Research Institute, South Korea. Relevant specimens are marked with circles on the bottom of the slides.

**Etymology:** The species-group name “*jangbogoensis*” is derived from the name of the Korean Antarctic Research Station, Jang Bogo Station, because the species was discovered near this station.

**Description** (Figs. 1A–F, 2 A–K, 3 A–H, 4 A–E, Table 1): Body size in vivo approximately  $95\text{--}135 \times 40\text{--}55 \mu\text{m}$  ( $n = 7$ ), on average  $97 \times 33 \mu\text{m}$  in protargol preparations; length:width ratio 3:1 on average (Table 1). Body outline

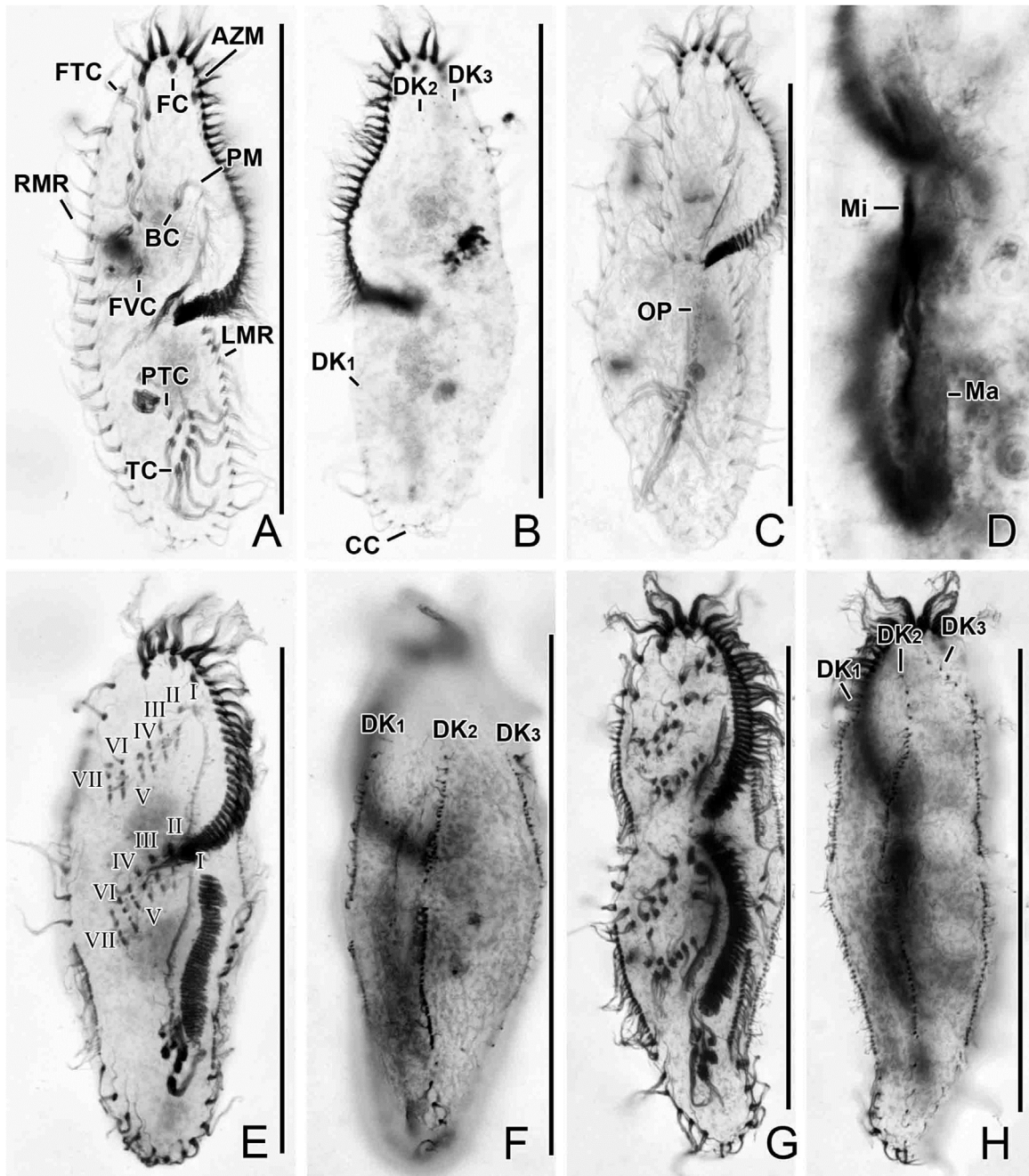


**Fig. 3.** A–H. Photomicrographs of *Gonostomum jangbogoensis* n. sp. after protargol preparation. **A, B:** Ventral and dorsal view of holotype. **C:** Ventral view of early divider. **D:** Dorsal view of late divider, showing macronuclear nodules and micronuclei. **E, F:** Ventral and dorsal view of a middle divider, showing the seven anlagen and dorsal kineties. **G, H:** Ventral and dorsal view of a late divider. AZM, adoral zone of membranelles; BC, buccal cirrus; CC, caudal cirri; DK<sub>1–3</sub>, dorsal kineties; FC, frontal cirri; FTC, frontoterminal cirri; FVC, frontoventral cirri; I–VII, frontoventral transverse anlagen I–VII; LMR, left marginal row; Ma, macronucleus nodule; Mi, micronuclei; OP, oral primordium; PM, paroral membrane; PTC, pretransverse cirri; RMR, right marginal row; TC, transverse cirri. Scale bars: 100 µm.

elliptical in vivo, both ends slightly narrowed. Body flexible, but not distinctly contractile, dorsoventrally flattened (Figs. 1A, B, E, F, 2 A–F, 3 A, B). Nuclear apparatus in central body portion, usually somewhat left of midline, composed of two ellipsoidal (8–22 × 5–12 µm in protargol preparations) macronuclear nodules and 1–3 micronuclei; in specimens with one micronucleus, never in-between the nodules. Con-

tractile vacuole posterior to buccal vertex, approximately 20 µm in diameter at end of diastole, no distinct collecting canals recognizable (Figs. 1B, 2 B). Cytoplasm grayish at low magnification. Cortical granules rod-shaped, colorless, 2.0–2.5 × 0.5–0.7 µm (Figs. 1C, D, 2 I). Locomotion without peculiarities, usually moderately fast creeping on bottom of Petri dish.

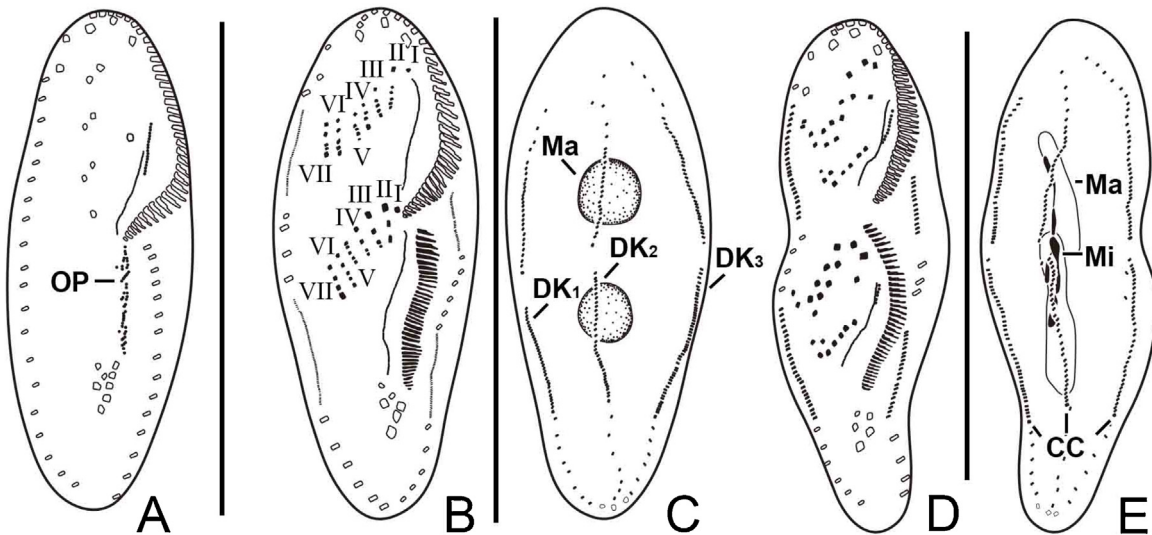


**Fig. 4.** A–E. Morphogenesis of *Gonostomum jangbogoensis* n. sp. after protargol preparation. A: Ventral view of early divider. B, C: Ventral and dorsal view of a middle divider. D, E: Ventral and dorsal view of a late divider. CC, caudal cirri; DK<sub>1–3</sub>, dorsal kineties; I–VII, frontoventral transverse anlagen I–VII; Ma, macronucleus nodule; Mi, micronuclei; OP, oral primordium. Scale bars: 100 µm.

Oral apparatus in *Gonostomum* pattern (Berger 2011). Adoral zone terminates at 52% of body length on average in protargol preparations, composed of 32–41, on average 37, membranelles; base of largest membranelles 6.2 µm wide on average, cilia of membranelles up to 20 µm long. Endoral commences at level of buccal cirrus, composed of densely spaced monokinetids (Figs. 1A, B, E, 2C, D, I, J, 3A). Paroral composed of 17–23 monokinetids, cilia 10–14 µm long. Pharyngeal fibers ordinary.

Frontal, transverse and caudal cirri approximately 20 µm long in vivo; remaining cirri about 15 µm long (Figs. 1A, 2C, D, G, H, 3A). Three frontal cirri slightly enlarged, two frontoterminal cirri at anterior end of right marginal row; buccal cirrus slightly anterior to level of distal end of endoral membrane (Figs. 1A, E, 2I, J, 3A). Usually three frontoventral cirral pairs slightly right of or in cell midline; cirrus III/2 slightly more anteriorly than posterior frontoterminal cirrus. Posteriormost frontoventral cirrus about at level of rear end of paroral. Six or seven transverse cirri arranged in hook-shaped pattern, rightmost transverse cirrus displaced slightly anteriorly; two pretransverse cirri form oblique pseudorow near transverse cirri. Right marginal row commences dorsolaterally at level of posterior frontoterminal cirrus, composed of 18–26, on average 21, cirri. Left marginal row begins left of proximal portion of adoral zone, composed of 13–19, on average 16, cirri; both marginal rows never connected posteriorly (Figs. 1A, E, 2H, 3A, Table 1).

Three bipolar dorsal kineties, bristles approximately 5 µm long in vivo; dorsal kinety 1 distinctly shortened anteriorly; three caudal cirri (Figs. 1F, 2F, 3B, Table 1).

**Ontogenesis of *Gonostomum jangbogoensis* n. sp.:** The formation of the oral primordium begins with apokinetal proliferation of basal bodies below the buccal vertex (Figs. 3C, 4A). The differentiation of adoral membranelles commences

in the anterior portion of the oral primordium and proceeds posteriadly while the anlage for the undulating membranes forms a longitudinal dikinetidal line of basal bodies to the right of the differentiating adoral zone (Figs. 3E, 4B). The parental adoral membranelles are retained (Figs. 3E, 4B, D).

Seven cirral streaks (= frontal-ventral-transverse cirral anlagen) are formed in both the proter and the opisthe; however, it is unclear whether these streaks originate from so-called primary primordia (Figs. 3E, 4B). A single out of 21 individuals has seven transverse cirri; a divider with eight streaks was not found.

The development of marginal rows and dorsal kineties proceeds as in congeners: the anlagen form within the parental structures of marginal rows, and dorsal kineties originate by intrakinetal proliferation of basal bodies, that is, two anlagen develop from each parental row. Each dorsal kinety will produce one caudal cirrus in the late stage of cell division. Parental structures are very likely resorbed (Figs. 3E–H, 4B–E). Based on the available dividers, it remains uncertain whether or not the two macronuclear nodules fuse into a single mass. In the late dividers, the micronuclei and macronuclear segments begin to divide (Figs. 3D, 4E).

**Phylogenetic analyses of *Gonostomum jangbogoensis* n. sp.:** The SSU rRNA gene sequence of *Gonostomum jangbogoensis* (GenBank accession number: MK860908) is 1346 bp in length, with a GC-content of 45.3%.

The present phylogeny of gonostomatids is far from robust, as indicated by the generally low support values. All *Gonostomum* species, except for *G. namibiense* and *G. paronense*, cluster together in a heterogenous clade, containing also *Cotterillia* and *Paragonostomoides*. *Gonostomum namibiense* and *G. paronense* branch before the *Gonostomum* spp. + *Paragonostomoides* + *Cotterillia* cluster. *Gonostomum jangbogoensis* n. sp. groups with *G. bromelicola* but this

**Table 1.** Morphometric data on protargol-impregnated specimens of *Gonostomum jangbogoensis* n. sp.

| Characteristic                              | Mean | SD   | SE  | CV   | Min  | M    | Max   | N  |
|---|------|------|-----|------|------|------|-------|----|
| Length, body                                | 97.7 | 7.2  | 1.7 | 7.4  | 84.2 | 97.6 | 115.8 | 19 |
| Width, body                                 | 33.1 | 4.8  | 1.1 | 14.6 | 26.3 | 33.5 | 45.7  | 19 |
| Ratio, body length: width                   | 3.0  | 0.3  | 0.1 | 11.0 | 2.2  | 3.0  | 3.4   | 19 |
| Length, adoral zone                         | 51.5 | 3.8  | 0.9 | 7.4  | 44.1 | 51.0 | 57.4  | 19 |
| Percentage, adoral zone length: body length | 52.8 | 3.4  | 0.8 | 6.4  | 47.1 | 52.6 | 59.0  | 19 |
| Length, largest membranelles                | 5.0  | 0.7  | 0.2 | 14.5 | 3.2  | 5.0  | 6.2   | 19 |
| Distance, anterior body end to RMR          | 13.5 | 4.1  | 0.9 | 30.4 | 7.2  | 12.8 | 22.5  | 19 |
| Distance, anterior body end to PM           | 26.5 | 2.8  | 0.7 | 10.8 | 20.4 | 26.9 | 31.8  | 19 |
| Distance, anterior body end to EM           | 31.1 | 4.2  | 1.0 | 13.6 | 24.9 | 31.1 | 41.3  | 19 |
| Distance, anterior body end to BC           | 26.3 | 2.4  | 0.6 | 9.3  | 21.9 | 26.4 | 30.4  | 19 |
| Distance, anterior body end to Ma           | 28.9 | 10.2 | 2.3 | 35.4 | 17.2 | 26.1 | 57.0  | 19 |
| Distance, posterior body end to TC          | 15.4 | 4.0  | 0.9 | 25.6 | 7.7  | 15.0 | 23.1  | 19 |
| Distance, anterior body end to RMR          | 3.4  | 1.3  | 0.3 | 38.7 | 1.0  | 3.1  | 6.0   | 19 |
| Distance, anterior body end to LMR          | 2.3  | 1.2  | 0.3 | 50.5 | 1.0  | 2.0  | 5.1   | 19 |
| Length, anterior Ma                         | 14.4 | 3.5  | 0.8 | 24.4 | 8.7  | 13.6 | 22.0  | 19 |
| Width, anterior Ma                          | 8.3  | 1.5  | 0.4 | 18.7 | 5.8  | 8.1  | 11.4  | 19 |
| Number, macronuclear nodules                | 1.9  | 0.3  | 0.1 | 16.6 | 1.0  | 2.0  | 2.0   | 19 |
| Length, micronuclei                         | 2.3  | 0.4  | 0.1 | 16.3 | 1.9  | 2.2  | 3.0   | 8  |
| Width, micronuclei                          | 2.1  | 0.3  | 0.1 | 12.4 | 1.8  | 2.1  | 2.5   | 8  |
| Micronucleus, number                        | 1.5  | 0.8  | 0.3 | 50.4 | 1.0  | 1.0  | 3.0   | 8  |
| Adoral membranelles, number                 | 37.3 | 2.6  | 0.6 | 6.9  | 32.0 | 37.0 | 41.0  | 19 |
| Frontal cirri, number                       | 3.0  | 0.0  | 0.0 | 0.0  | 3.0  | 3.0  | 3.0   | 19 |
| Frontoterminal cirri, number                | 2.0  | 0.0  | 0.0 | 0.0  | 2.0  | 2.0  | 2.0   | 19 |
| Buccal cirrus, number                       | 1.0  | 0.0  | 0.0 | 0.0  | 1.0  | 1.0  | 1.0   | 19 |
| Frontoventral cirral pairs, number          | 3.2  | 0.4  | 0.1 | 13.1 | 3.0  | 3.0  | 4.0   | 19 |
| Pretransverse cirri, number                 | 2.0  | 0.0  | 0.0 | 0.0  | 2.0  | 2.0  | 2.0   | 19 |
| Transverse cirri, number                    | 6.1  | 0.2  | 0.1 | 3.8  | 6.0  | 6.0  | 7.0   | 19 |
| Left marginal cirri, number                 | 16.1 | 1.4  | 0.3 | 8.9  | 13.0 | 16.0 | 19.0  | 19 |
| Right marginal cirri, number                | 21.7 | 1.8  | 0.4 | 8.4  | 18.0 | 21.0 | 26.0  | 19 |
| Caudal cirri, number                        | 3.0  | 0.0  | 0.0 | 0.0  | 3.0  | 3.0  | 3.0   | 19 |
| Paroral kinetids, number                    | 19.1 | 1.8  | 0.4 | 9.5  | 17.0 | 19.0 | 23.0  | 19 |
| Dorsal kineties, number                     | 3.0  | 0.0  | 0.0 | 0.0  | 3.0  | 3.0  | 3.0   | 19 |
| Dorsal kinety 1, number of bristles         | 32.5 | 2.1  | 0.5 | 6.3  | 29.0 | 32.0 | 37.0  | 19 |
| Dorsal kinety 2, number of bristles         | 27.7 | 2.5  | 0.6 | 9.0  | 23.0 | 27.0 | 32.0  | 19 |
| Dorsal kinety 3, number of bristles         | 31.1 | 2.6  | 0.6 | 8.3  | 26.0 | 31.0 | 35.0  | 19 |
| Dorsal bristles, total number               | 91.1 | 6.2  | 1.4 | 6.8  | 79   | 91   | 101   | 19 |

CV-coefficient of variation (%); M-median; Max-maximum; Mean-arithmetic mean; Min-minimum; N-number of specimens investigated; SD-standard deviation; SE-standard error of arithmetic mean.

BC, buccal cirrus; EM, endoral membrane; LMR, left marginal row; Ma, macronuclear nodules; PM, paroral membrane; RMR, right marginal row; TC, transverse cirri.

branching had low support in the BI analyses (posterior probability = 0.6) and the ML analyses (bootstrap value <50%) ([Fig. 5](#)).

Additionally, we tested three scenarios, 1) monophyly of gonostomatids (*Gonostomum* spp. + *Paragonostomoides* + *Cotterillia*); 2) monophyly of all *Gonostomum* species; and 3) monophyly of all *Gonostomum* spp., except for *G. namibense* and *G. paronense*. The first and last scenarios were not rejected ([Table 3](#)).

## Discussion

### Comparison with similar species

So far, seventeen species, including two invalid species, have been assigned to the genus *Gonostomum* (see introduction). Considering its elliptical body, two macronuclear nodules, cortical granules and more than 17 paroral kinetids, *Gonostomum jangbogoensis* n. sp. should be compared with

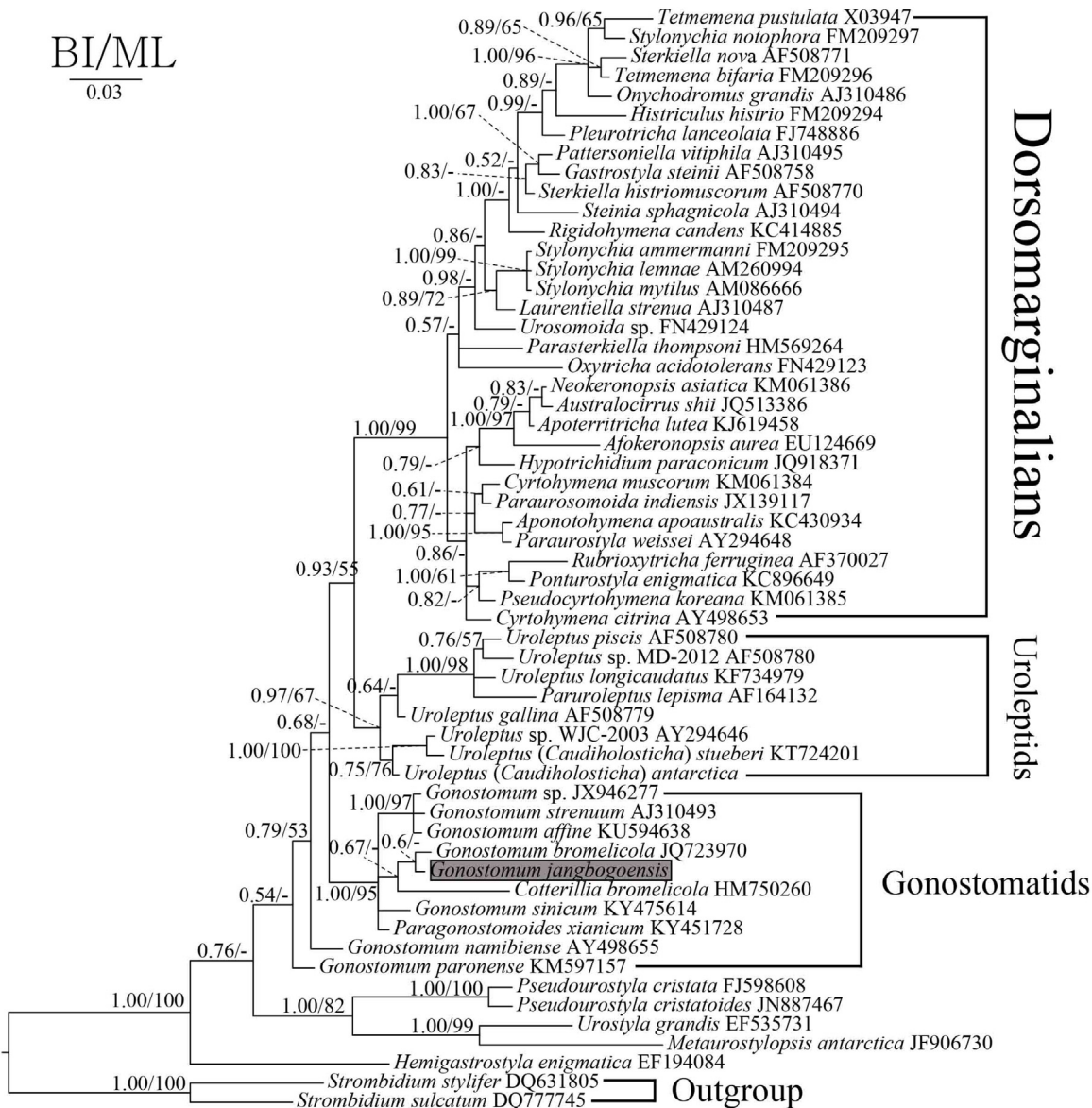


**Fig. 5.** Phylogenetic tree based on SSU rRNA gene sequences showing the position of *G. jangbogoensis* as determined by the Bayesian inference (BI) and Maximum Likelihood (ML) methods. Posterior probability values for the BI and bootstrap values for the ML are shown on nodes (for interpretation of values, see Material and Methods). Dashes denote bootstrap values <50% or different topologies in BI and ML phylogenies.

*Gonostomum* sp. 1 sensu Shin (1994), *G. bromelicola*, and *G. fraterculus* (Table 2). As shown in the ontogenesis, *G. jangbogoensis* can be easily separated by the additional frontal-ventral-transverse cirral anlage due to the formation of one (sometimes two) extra anlage(n) which forms a transverse cirrus and two frontoventral cirri (see below). *Gonostomum fraterculus* differs from *G. jangbogoensis* n. sp. mainly in the number of pretransverse and transverse cirri (7 vs. 8 or 9), and in their habitats (soil vs. freshwater) (Foissner 2016).

*Gonostomum bromelicola* can be separated from *G. jangbogoensis* n. sp. by the number of left marginal cirri (9–13 vs. 13–19), the number of paroral kinetids (11–17 vs. 17–23), the

length of paroral cilia (15–20 µm vs. 10–14 µm), the number of frontoventral cirral pairs (2 vs. 3 or 4), the number of pretransverse and transverse cirri (7 vs. 8 or 9), the dorsal kinety 2 (distinct break/irregularities vs. ordinary course), by the size and arrangement of the rod-shaped cortical granules (3.0–4.0 × 1.0 µm, scattered and in short rows vs. 2.0–2.5 × 0.5–0.7 µm, irregularly distributed) and the habitat (tanks of bromeliads vs. freshwater) (Foissner 2016).

*Gonostomum* sp. 1 described by Shin (1994) can be distinguished from *G. jangbogoensis* n. sp. by the number of pretransverse and transverse cirri (6 or 7 vs. 8 or 9), and habitat (soil vs. freshwater).

**Table 2.** Comparison of morphological features in *Gonostomum jangbogoensis* n. sp. with closely related species.

| Characteristic                             | <i>G. sp. 1</i> | <i>G. bromelicola</i>   | <i>G. fraterculus</i>                        | <i>G. jangbogoensis</i> n. sp.                                      |
|--|-----------------|---|--|---|
| Body length (stained), $\mu\text{m}$       | 87–155          | 75–95   | 77–116                                       | 84–116  |
| Cortical granules (shape and size)         | Not mentioned   | Present (rod-shaped, $3.0\text{--}4.0 \times 1 \mu\text{m}$ ) | Possibly present (colourless, inconspicuous) | (rod-shaped, $2.0\text{--}2.5 \times 0.5\text{--}0.7 \mu\text{m}$ ) |
| Adoral membranelles, number                | 32–43           | 34–43   | 31–43  | 32–41   |
| Frontal cirri, number                      | 3               | 3   | 3  | 3   |
| Frontoterminal cirri, number               | 2               | 2   | 2  | 2   |
| Right marginal cirri, number               | 16–29           | 15–22   | 17–30  | 18–26   |
| Left marginal cirri, number                | 12–20           | 9–13  | 12–21  | 13–19   |
| Pretransverse and transverse cirri, number | 6 or 7          | 7   | 7  | 8 or 9  |
| Frontoventral cirral pair, number          | 3 <sup>a</sup>  | 2   | 2  | 3 or 4 <sup>b</sup>   |
| Dorsal kineties, number                    | 3               | 3   | 3  | 3   |
| Paroral kinetids, number                   | 19–33           | 11–17   | 17–28  | 17–23   |
| Caudal cirri, number                       | 2 or 3          | 2 or 3  | 3  | 3   |
| Habitat                                    | Soil            | In tanks of bromeliads  | Soil   | Freshwater  |
| Data source                                | Shin (1994)     | Foissner (2016)   | Foissner (2016)                              | Present study   |

<sup>a</sup>Shin (1994) reported 8 or 9 (usually 9) frontoventral cirri including the cirrus III/2 and 2 frontoterminal cirri.

<sup>b</sup>Cirrus III/2 not included.

**Table 3.** Tree topology tests with log likelihoods and *p*-values from approximately unbiased (AU), weighted Shimodaira-Hasegawa (WSH), and weighted Kishino-Hasegawa (WKH) tests on phylogenetic trees.

| Topology  | Log likelihood | Difference to best tree | AU ( <i>p</i> ) | WSH ( <i>p</i> ) | WKH ( <i>p</i> ) | Conclusion   |
|---|----------------|-------------------------|-----------------|------------------|------------------|--------------|
| Monophyly of gonostomatids ( <i>Gonostomum</i> spp. + <i>Cotterillia</i> + <i>Paragonostomoides</i> ) | −5761.728      | 0.000                   | 0.883           | 0.939            | 0.863            | Not rejected |
| Monophyly of all <i>Gonostomum</i> spp.   | −5782.065      | 20.337                  | 0.003           | 0.029            | 0.017            | Rejected     |
| Monophyly of all <i>Gonostomum</i> spp. except for <i>G. namibiense</i> and <i>G. paronense</i>       | −5770.768      | 9.040                   | 0.137           | 0.228            | 0.137            | Not rejected |

*Gonostomum namibiense* has also rod-shaped cortical granules. It differs from *G. jangbogoensis* n. sp. mainly in the shape of the posterior body portion (tail-like vs. rounded), the size of the rod-shaped cortical granules ( $1.0 \times 0.3 \mu\text{m}$  vs.  $2.0\text{--}2.5 \times 0.5\text{--}0.7 \mu\text{m}$ ), the number of paroral kinetids (5–18 vs. 17–23) and transverse cirri (0–5 vs. 6–7) (Foissner et al. 2002).

Both species of the genus *Apogonostomum* Foissner, 2016, *A. pantanalense* Foissner, 2016 and *A. vleiacola* Foissner, 2016, have rod-shaped cortical granules. *Apogonostomum pantanalense* differs from *G. jangbogoensis* n. sp. by the size of rod-shaped cortical granules ( $6.0 \times 1.0 \mu\text{m}$  vs.  $2.0\text{--}2.5 \times 0.5\text{--}0.7 \mu\text{m}$ ), the shape of the posterior body portion (tail-like vs. rounded), and the caudal cirri (absent vs. present) (Foissner 2016).

*Apogonostomum vleiacola* is similar to *G. jangbogoensis* n. sp. with respect to the size of the rod-shaped cortical granules. However, *Apogonostomum vleiacola* can be separated from *G. jangbogoensis* by caudal cirri (absent vs. present), shape of the posterior body end (tail-like vs. rounded), and the number of adoral membranelles (44–64 vs. 32–41) (Foissner 2016).

### Morphogenetic comparison

Since some stages of *G. jangbogoensis* n. sp. of early to middle dividers were not available, we could not determine whether (1) anlage I develops separately and (2) the two macronuclear nodules fuse into a single mass. Morphogenesis has been reported for six *Gonostomum* species so far:

*G. affine*, *G. algicola*, *G. kuehnelti*, *G. strenuum*, *G. sinicum*, and *G. singhii* (Berger 1999, 2011; Eigner 1999; Lu et al. 2017).

Considering the morphogenesis of these six species, the norm is six cirral anlagen. However, *G. jangbogoensis* n. sp. has at least one additional anlage, that is, seven or eight cirral anlagen in specimens which form seven transverse cirri. Even though we identified seven anlagen in dividers, our interphasic specimens suggest that some individuals have eight anlagen because they had one additional frontoventral cirral pair and/or transverse cirrus. In the *G. affine* complex, two specimens of Eigner's population (1999, Table 1, p. 36) have an anlage VII (in proter and/or opisthe). *Gonostomum* sp. 1 of Shin (1994) usually has two more frontal-ventral-transverse (FVT) cirri than a typical 18 FVT-cirri hypotrich, that is, it displays seven anlagen. According to Berger (2011), the extra cirri obviously result from one additional anlage. The populations collected from Korea (Shin 1994) and Antarctica (this study) prove that this character state (one additional cirral anlage) is stable across the populations though they are located very far away from each other.

## Phylogenetic analyses

According to our phylogenetic analyses based on the SSU rRNA gene (Fig. 5), the *Gonostomum* species sequenced to date have emerged from a node of soft polytomy, which also comprises *Cotterillia bromelicola*, *Paragonostomoides xianicum*, and a cluster composed of some other *Gonostomum* species. The monophly of gonostomatids is highly supported by BI and ML trees (BI/ML, 1.00/95) except for *G. namibiense* and *G. paronense*. The monophly of all gonostomatids was not rejected based by the tree topology test. However, the branch of *G. namibiense* and *G. paronense* was separated from the major cluster of other gonostomatid species but with poor statistical support. According to Lu et al. (2017), both *G. namibiense* and *G. paronense* belong to *Apogonostomum*, due to their tailed bodies and frontoventral cirral pairs extending from the mid-body to the buccal vertex or to transverse cirri (Bharti et al. 2015). *Gonostomum jangbogoensis* n. sp. is closely related to *G. bromelicola* in our phylogenetic tree but they clearly differ in that *G. bromelicola* has a fragmented dorsal kinety 2 (Foissner 2016).

## Author contributions

J.K. collected the samples and K.P. carried out all laboratory work (culture, analysis, illustrations, calculations, etc.). K.P., J.J., G.M., and S.K. wrote the manuscript. All authors read and approved the final manuscript.

## Acknowledgements

This work was supported by the Korea Polar Research Institute [research grant PE19150 and PE20150].

## References

- Alfaro, M.E., Zoller, S., Lutzoni, F., 2003. Bayes or bootstrap? A simulation study comparing the performance of Bayesian Markov Chain Monte Carlo sampling and bootstrapping in assessing phylogenetic confidence. Mol. Biol. Evol. 20, 255–266.
- Berger, H., 1999. Monograph of the Oxytrichidae (Ciliophora, Hypotrichia). Monogr. Biol. 78, 1–1080.
- Berger, H., 2011. Monograph of the Gonostomatidae and Kahliellidae (Ciliophora, Hypotrichia). Monogr. Biol. 90, 1–741.
- Berger, H., Foissner, W., 2003. Illustrated guide and ecological notes to ciliate indicator species (Protozoa, Ciliophora) in running waters, lakes, and sewage plants. In: Steinberg, W., Calmano, K. (Eds.), Handbuch Angewandte Limnologie, 17. ErgLfg, pp. 1–160, Ecomed, Landsberg am Lech (now available at Wiley).
- Bharti, D., Kumar, S., La Terza, A., 2015. Two gonostomatid ciliates from the soil of Lombardia, Italy; including note on the soil mapping project. J. Euk. Microbiol. 62, 762–772.
- Darriba, D., Taboada, G., Doallo, R., Posada, D., 2012. jModelTest 2: more models, new heuristics and parallel computing. Nat. Methods 9, 772.
- Eigner, P., 1999. Comparison of divisional morphogenesis in four morphologically different clones of the genus *Gonostomum* and update of the natural hypotrich system (Ciliophora, Hypotrichida). Eur. J. Protistol. 35, 34–48.
- Engelmann, T.W., 1862. Zur Naturgeschichte der Infusionsthiere. Z. Wiss. Zool. 11, 347–393.
- Foissner, W., 1987. Neue und wenig bekannte hypotrichische und colpodide Ciliaten (Protozoa: Ciliophora) aus Österreich und Deutschland. Sber. öst. Akad. Wiss. Mathematisch-naturwissenschaftliche Klasse, Abt I 195 (year 1986), 217–268.
- Foissner, W., 1998. An updated compilation of world soil ciliates (Protozoa, Ciliophora), with ecological notes, new records, and descriptions of new species. Eur. J. Protistol. 34, 195–235.
- Foissner, W., 2014. An update of ‘basic light and scanning electron microscopic methods for taxonomic studies of ciliated protozoa’. Int. J. Syst. Evol. Microbiol. 64, 271–292.
- Foissner, W., 2016. Terrestrial and semiterrestrial ciliates (Protozoa, Ciliophora) from Venezuela and Galápagos. Denisia 35, 1–912.
- Foissner, W., Agatha, S., Berger, H., 2002. Soil ciliates (Protozoa, Ciliophora) from Namibia (Southwest Africa), with emphasis on two contrasting environments, the Etosha region and the Namib Desert. Part I: Text and line drawings. Part II: Photographs. Denisia 5, 1–1459.
- Foissner, W., Blatterer, H., Berger, H., Kohmann, F., 1991. Taxonomische und ökologische Revision der Ciliaten des Saprobiensystems – Band I: Cyrtophorida, Oligotrichida, Hypotrichia, Colpodea. Informationsberichte Bayer. Landesamt für Wasserwirtschaft 1/91, pp. 1–478.
- Gellért, J., 1942. Életégyüttes a fakéreg zöldporos bevonatában (Lebensgemeinschaft in dem grünpulverige Überzug der Baumrinde). Univ. Francisco-Josephina. Kolozsvár. Acta Sci. Math. Nat. 8, 1–36.
- Guindon, S., Dufayard, J.F., Lefort, V., Anisimova, M., Hordijk, W., Gascuel, O., 2010. New algorithms and methods to estimate maximum-likelihood phylogenies: assessing the performance of PhyML 3.0. Syst. Biol. 59, 307–321.

- Hall, T., 1999. BioEdit: a user-friendly biological sequence alignment editor and analysis program for Windows 95/98/NT. *Nucleic Acids Symp. Ser.* 41, 95–98.
- Hillis, D.M., Bull, J.J., 1993. An empirical test of bootstrapping as a method for assessing confidence in phylogenetic analysis. *Syst. Biol.* 42, 182–192.
- ICZN (The International Commission on Zoological Nomenclature), 2012. Amendment of Articles 8, 9, 10, 21 and 78 of the International Code of Zoological Nomenclature to expand and refine methods of publication. *Bull. Zool. Nomencl.* 69, 161–169.
- Jeanmougin, F., Thompson, J., Gouy, M., Higgins, D., Gibson, T., 1998. Multiple sequence alignment with clustal X. *Trends Biochem. Sci.* 23, 403–405.
- Jiang, Y., Yang, E.J., Min, J.O., Kang, S.H., Lee, S.H., 2013. Using pelagic ciliated microzooplankton communities as an indicator for monitoring environmental condition under impact of summer sea-ice reduction in western Arctic Ocean. *Ecol. Indic.* 34, 380–390.
- Jiang, Y., Xu, H., Hu, X., Zhu, M., Al-Rasheid, K.A.S., Warren, A., 2011. An approach to analyzing spatial patterns of planktonic ciliate communities for monitoring water quality in Jiaozhou Bay, northern China. *Mar. Pollut. Bull.* 62, 227–235.
- Jung, J.-H., Baek, Y.-S., Kim, S., Choi, H.-G., Min, G.-S., 2011. A new marine ciliate, *Metaurostylopsis antarctica* nov. spec. (Ciliophora, Urostylida) from the Antarctic Ocean. *Acta Protozool.* 50, 289–300.
- Kim, M., Cho, A., Lim, H.S., Hong, S.G., Kim, J.H., Lee, J., Choi, T., Ahn, T.S., Kim, O.S., 2015. Highly heterogeneous soil bacterial communities around Terra Nova Bay of northern Victoria Land, Antarctica. *PLoS One* 10, e0119966.
- Lu, X., Huang, J., Shao, C., Al-Farraj, S.A., Gao, S., 2017. Morphology and morphogenesis of a novel saline soil Hypotrichous ciliate, *Gonostomum sinicum* nov. spec. (Ciliophora, Hypotrichia, Gonostomatidae), including a report on the small subunit rDNA sequence. *J. Euk. Microbiol.* 64, 632–646.
- Lynn, D.H., 2008. The Ciliated Protozoa: Characterization, Classification, and Guide to the Literature, 3rd ed. Springer, Dordrecht.
- Pan, X., Bourland, W.A., Song, W., 2013. Protargol synthesis: an in-house protocol. *J. Euk. Microbiol.* 60, 609–614.
- Ronquist, F., Teslenko, M., van der Mark, P., Ayres, D.L., Darling, A., Höhna, S., Larget, B., Liu, L., Suchard, M.A., Helsenbeck, J.P., 2012. MrBayes 3.2: efficient Bayesian phylogenetic inference and model choice across a large model space. *Syst. Biol.* 61, 539–542.
- Russell, P.J., Hertz, P.E., McMillan, B., 2016. Biology: the Dynamic Science, 4rd ed. Cengage Learning.
- Shimodaira, H., Hasegawa, M., 2001. CONSEL: for assessing the confidence of phylogenetic tree selection. *Bioinformatics* 17, 1246–1247.
- Shin, M.K., 1994. Systematics of Korean Hypotrichs (Ciliophora, Polyhymenophora, Hypotrichida) and Molecular Evolution of Hypotrichs. PhD Dissertation, Seoul National University, Seoul, Korea. Dissertation Seoul National University.
- Small, E.B., Lynn, D.H., 1985. Phylum Ciliophora Doflein, 1901. In: Lee, J.J., Hutner, S.H., Bovee, E.C. (Eds.), An Illustrated Guide to the Protozoa. Lawrence, Society of Protozoologists, pp. 393–575.
- Sonnenberg, R., Nolte, A.W., Tautz, D., 2007. An evaluation of LSU rDNA D1-D2 sequences for their use in species identification. *Front. Zool.* 4, 6.
- Stein, F., 1859. Der Organismus der Infusionsthiere nach eigenen Forschungen in systematischer Reihenfolge Bearbeitet. I. Abtheilung. Allgemeiner Theil und Naturgeschichte der hypotrichen Infusionsthiere. Engelmann, Leipzig.
- Sterki, V., 1878. Beiträge zur Morphologie der Oxytrichinen. *Z. Wiss. Zool.* 31, 29–58.
- Swofford, D., 2003. PAUP\*: Phylogenetic Analysis Using Parsimony (\* and Other Methods).
- Vd'acný, P., Rajter, L., 2015. Reconciling morphological and molecular classification of predatory ciliates: evolutionary taxonomy of dileptids (Ciliophora, Litostomatea, Rhynchostomatia). *Mol. Phylogenet. Evol.* 90, 112–128.
- Vd'acný, P., Tirjaková, E., 2006. A new soil hypotrich ciliate (Protozoa, Ciliophora) from Slovakia: *Gonostomum albicarpathicum* nov. spec. *Eur. J. Protistol.* 42, 91–96.
- Vincent, W.F., James, M.R., 1996. Biodiversity in extreme aquatic environments: lakes, pond and streams of Ross Sea sector, Antarctica. *Biodivers. Conserv.* 5, 1451–1471.
- Wang, J., Ma, J., Qi, S., Shao, C., 2017. Morphology, morphogenesis and molecular phylogeny of a new soil ciliate *Paragonostomoides xianicum* n. sp. (Ciliophora, Hypotrichia, Gonostomatidae). *Eur. J. Protistol.* 61, 233–243.
- Xu, H., Zhang, W., Jiang, Y., Yang, E.J., 2014. Use of biofilm-dwelling ciliate communities to determine environmental quality status of coastal water. *Sci. Total Environ.* 470–471, 511–518.